

HIGH-TEMPERATURE EXPERIMENTS ON MODEL –SCALE CONCRETE SLABS AT HIGH DISPLACEMENT

Samantha J. FOSTER ¹, Ian W. BURGESS and Roger J. PLANK

*University of Sheffield, Mappin Street, Sheffield S1 3JD, United Kingdom
(¹s.j.foster@sheffield.ac.uk)*

ABSTRACT

Large-scale fire tests in the multi-storey steel framed building at Cardington have shown large reserves of fire resistance in unprotected composite floor systems. These tests showed that the floor system does not collapse, even at very large deformations. The enhanced resistance is attributed to membrane forces which assist in maintaining the structural integrity through diaphragm action. The Building Research Establishment in the UK has since developed a new design method for composite floors in fire, based on a simplified model of the membrane action of rectangular slabs. Small-scale tests have been carried out at ambient temperature, and the experimental results compare well with the design method and are generally conservative. The experimental work has recently been extended to tests of loaded small-scale slabs at elevated temperatures. This paper presents the results from a number of such tests conducted on horizontally unrestrained slabs. The purpose of these tests is to investigate the influence of thermal curvature on the failure mechanisms of rectangular slabs, since this is not explicitly allowed for in the simplified design method. The more detailed issues being studied include the effects of reinforcement percentage and reinforcement bond strength at high temperatures on the final integrity failure due to tensile cracking. Observations from the high-temperature tests have shown that the mechanism of failure differs from that assumed in the simplified design method. The observed slab behaviour at high temperatures is that high double-curvature deflection is created quickly, and this leads to full-depth cracking across the short span of the slab, but the association with a yield-line mechanism is much less obvious. Some numerical modelling studies have accompanied the testing, and comparisons have been made with the simplified design method.

KEYWORDS: *Tensile membrane action, reinforced concrete slabs, fire performance, high temperature experiments*

INTRODUCTION

During 1995 and 1996, six localised fire tests [1] were conducted on the full-scale, eight storey, steel-framed building at the Building Research Establishment's Cardington Laboratory. These large-scale fire tests were conducted to investigate the behaviour of compartments of different sizes at various locations within the building. These tests have shown that unprotected composite floor slabs have large reserves of fire resistance. The enhanced fire resistance is attributed to membrane forces which assist in maintaining the structural integrity through diaphragm (or tensile membrane) action.

Current structural fire design codes [2] assume that a composite slab acts as a one-way spanning beam between parallel secondary beams, resisting loads through bending and shear, and as the compression flange of the composite beams themselves. Although this design method is simple, it ignores any beneficial effect deriving from tensile membrane action in the floor slabs at large displacements. This implies that the current codified design method is not addressing the true structural behaviour of the building during a fire.

Significant experimental and theoretical work [3-7] has been carried out on the behaviour of concrete floor slabs at ambient temperature when subject to large deflections. The work showed that the concrete slabs could support loads in excess of the well-known yield-line failure load. The mechanism of the enhancement was shown to be tensile membrane action, which can form within the slab irrespective of whether its boundaries are restrained or unrestrained in the horizontal sense.

Following the fire tests at Cardington a simplified design method [8] was developed based on principles taken from previous research work on tensile membrane action carried out in the late 1960s. The simple design method was a significant improvement on previous methods, which were limited to flexural behaviour. The new design method divides the floor system into square or rectangular slab panels, which are surrounded by protected support beams which usually lie on the column grid-lines. During the late stages of a fire the applied load is mainly supported by membrane action in the composite slab. One of the major assumptions in the design method is that the slab reinforcement over the protected beams fractures during the fire due to a combination of high hogging curvature and membrane tension. This assumption is conservative since, if the reinforcement were to remain intact, the induced tensile membrane forces within the slab would be much higher. A slab is assumed to be horizontally unrestrained, so that the tension field in the central region of the slab is balanced only by the compressive in-plane forces around its perimeter. This simple design method was initially limited to isotropic reinforcement, but has recently been extended to incorporate orthotropic arrangements of reinforcement [9-10]. A series of experiments was conducted by the author on horizontally unrestrained concrete slabs, with both isotropic and orthotropic reinforcement. The influence of bond was investigated by comparing the results from slabs using smooth and deformed (ribbed) reinforcing bars. The slabs were tested at ambient temperature to verify the assumptions made in the simple design method. However, it can not be assumed that the basic behaviour observed at ambient temperature will necessarily remain the same at elevated temperatures. The test series has been extended to investigate the slab and bond behaviour under elevated temperatures, in order to further understand the mechanics of the membrane action and to provide comparisons with the simple design method.

This paper presents the results from the first series of experiments on horizontally unrestrained concrete slabs with varying percentages of isotropic reinforcement, under elevated temperatures. Further tests will be carried out on orthotropic reinforcement at a later stage. The influence of bond between the reinforcement bars and concrete at elevated

temperature is considered by comparing the results from slabs using smooth and deformed (ribbed) reinforcing bars.

SIMPLE DESIGN METHOD

The new equilibrium method considers a mode of failure that was observed in many ambient-temperature tests, mainly conducted on flat slabs, whose cracking pattern is illustrated in Fig. 1.

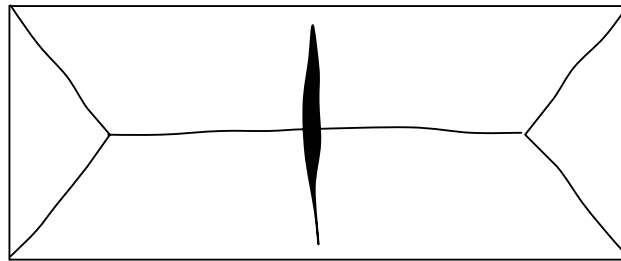


FIGURE 1: Cracking pattern observed in slabs due to tensile membrane action.

The typical model of failure in these tests, following tensile membrane action, was due to localised cracking through the full depth of the slab forming across the shorter span. This resulted in reinforcement fracture along these cracks and, although structural stability was not generally lost, the integrity of the fire compartmentation was breached.

The full derivation of the simple design method for isotropic and orthotropic reinforcement has been published [9] and will not be repeated here. The simple design method for fire conditions is based on rigid-plastic behaviour with the assumption that the mode of failure remains the same as at ambient temperature.

NUMERICAL MODELLING

Numerical studies have been carried out using the University of Sheffield software *Vulcan*. The numerical software has been developed over recent years for 3-D analysis of the structural behaviour of composite and steel-famed buildings in fire [11-12]. *Vulcan* uses the Mindlin/Reissner (thick plate) theory, and thermal expansion, cracking, geometric and material non-linearities are taken into account. Three dimensional models have been created of the model-scale slabs (Fig. 2).

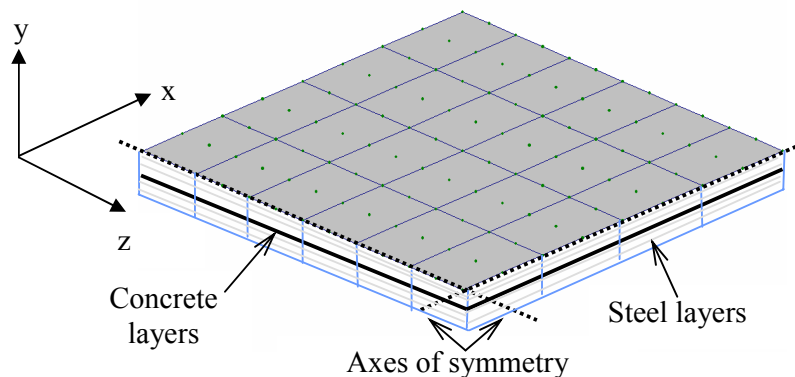


FIGURE 2 : Typical configuration of model-scale slab mesh

The concrete elements used are quadrilateral 9-noded shell elements. The slab elements are sub-divided into 10 layers of which 8 layers represent the concrete and two layers the steel reinforcement. The reordered temperatures through the depth of the slab have been used to calculate the temperature history for each layer. The reinforcing steel bars are modelled by a smeared layer approach, the thickness of the layer being set so that its cross-sectional area is equal to the total cross-sectional area of slab reinforcement and the layer's stress properties are set as uniaxial in the direction of the bars. Perfect bond is assumed between the reinforcing steel layers and the surrounding concrete. The Eurocode 4 part 1.2 [13] concrete material properties were used together with the concrete strengths measured on the day of the test and the yield strength of the reinforcing wire.

TEST CONFIGURATION AND INSTRUMENTATION

Two sizes of slab were tested, whose nominal dimension (in mm) were 920x620x15 and 920x620x22, with the supported area being 850x550. The actual depth of the slab varied slightly between tests, and measurements were made after each test. The test setup in these experiments is very similar to the previous tests at ambient temperature [10]. The slabs were tested in a loading rig in which constant loads were maintained at 12 points (Fig. 3).

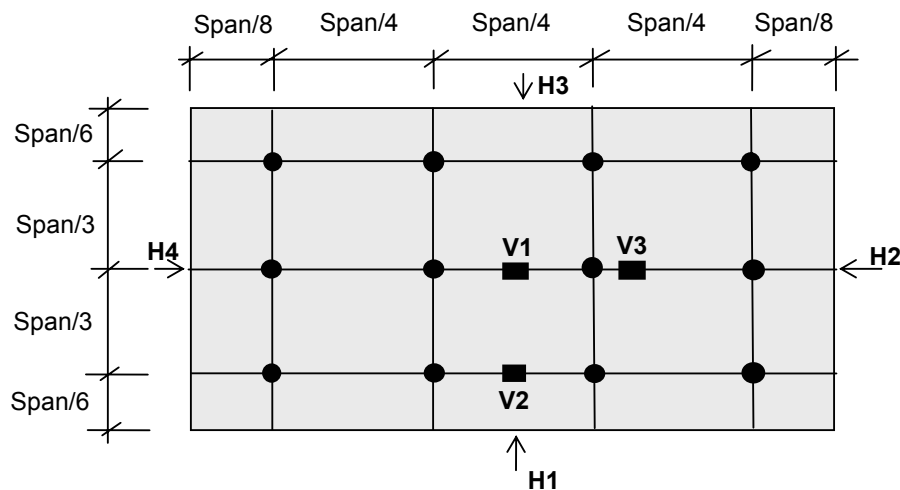


FIGURE 3 : Location of applied loading and displacement gauges

The loading frame and test set-up is shown in Fig. 4. The applied load remained vertical with the aid of ball-joints which allowed the loading system to rotate as the slab deflected. The slab was placed on a supporting frame, providing vertical support around the perimeter.



FIGURE 4 : Typical arrangement of test set-up and supporting frame

The four corners of the slab were loosely clamped to restrain vertical upward movement, but no horizontal restraint was provided at the supported edges. The heating device was constructed from a steel box lined with insulation board to increase the heating rate and protect the steel casing. Heating was generated by four electrical elements within the steel box. Fig. 5 shows the heating elements and supporting frame.



FIGURE 5 : Arrangement of heating elements

The slabs were reinforced with 0.71mm diameter smooth or deformed (ribbed) steel wire, distributed isotropically. The deformed wire was made by indenting the smooth wire using a purpose-built machine. The indentations had the effect of increased bond between the concrete and reinforcement but also reduced the reinforcement's ductility; the tested ductility for smooth wire was 20.3%, reducing to 11.4% for deformed wire. The percentage of reinforcement in any slab cross-section varied between 0.05% and 0.25%. The concrete mix was composed of gritty sand with fine aggregate ranging between 1 and 4mm, a cement-sand ratio of 1:3, and a water-cement ratio of 0.47. The measured yield strength of reinforcement and the compressive strength of concrete are shown in Table 1 in the Appendix.

The logged instrumentation included a load cell and several displacement transducers to measure both the horizontal and vertical displacements during the test (Fig. 4). The temperatures of the underside, reinforcement level and topside of the slab were measured with 12 thermocouples placed at key locations. The thermocouples measured temperatures through the depth of the slab, being placed at 4 locations, on 3 levels through the slab. Fig. 6 shows the temperature growth at these locations and levels for a typical test. The temperatures show consistency between the readings at the different positions at each of the levels through the slab.

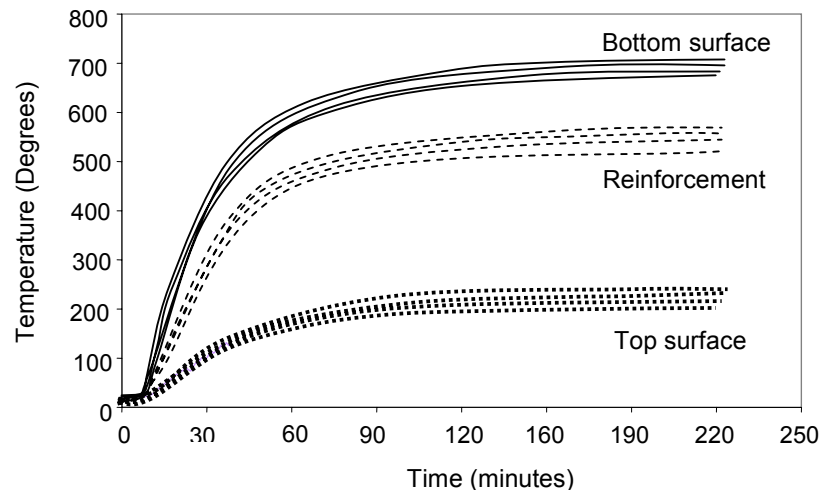


FIGURE 6 : Temperature profiles

OBSERVATIONS OF SLAB BEHAVIOUR

The slabs were subjected to the imposed load before the heating elements were switched on. They were tested in the sequence shown in Table 1. Test 1 has not been included, as it was used only to check the temperature distributions in the slab at various key locations. Test 3 was a re-test of Slab 2, which had been lightly loaded and showed little damage although it had some residual distortion. The fourteen slabs all behaved similarly. Approximately 10-15 minutes after the furnace was switched on, diagonal cracks occurred across the corners as the slab deflected into double curvature. After 20 minutes, a single transverse crack could be seen forming on the topside of the slab in its central region. Over time this crack developed outwards in the transverse short-span direction towards the long edges of the slab (Fig. 7).



FIGURE 7 : Test 7: View of the topside of slab after test.

Most of the slabs developed crack patterns resembling a yield line mechanism towards the end of the test, usually occurring after about 2 hours. The crack patterns resemble those of similar slabs tested at ambient temperature [10], except that the diagonal yield lines tended to align more in the long direction of the slab (Fig. 8(a)), giving a much shorter central yield line than usual. In Test 6, which was lightly reinforced and lightly loaded, diagonal cracking was only apparent after cooling (Fig. 8(b)). The formation of these yield lines seems to depend on the applied load level, while the development of the initial transverse crack after the slab deflects into double curvature is associated with its thermal bowing.

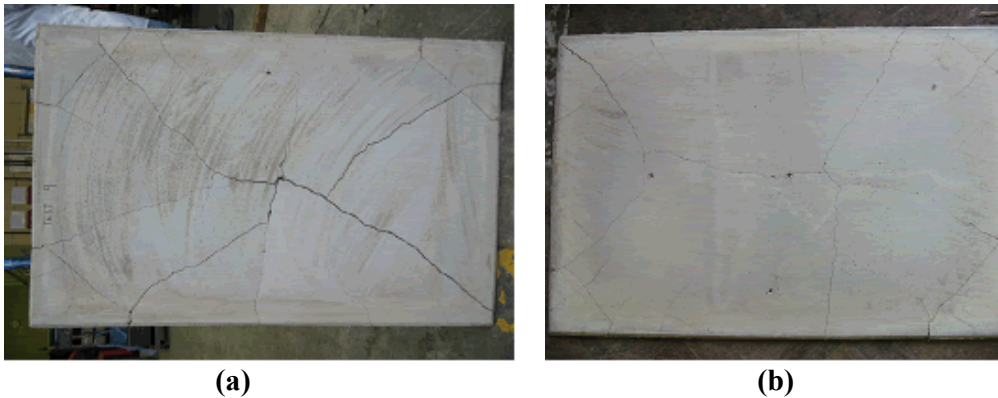


FIGURE 8 : View of bottom of slab; (a) Test 9, (b) Test 6, after testing.

The bond strength between reinforcement and concrete appeared [10] to be a major contribution to the failure of the slab at ambient temperature. At elevated temperatures, the influence of bond dominates the slab failure. For comparison, Fig. 9 shows photographs taken immediately after Tests 12 and 13. These tests were identical, the slabs having the same reinforcement percentages (0.25% in any cross-section) and imposed load; the only difference being the reinforcement type. In Test 12, deformed wire was used, and it can be

seen in Fig. 9 that the transverse crack has opened because the reinforcement across it has fractured. The slab in Test 13, reinforced with smooth wire, shows a transverse crack which re-closed after the test.

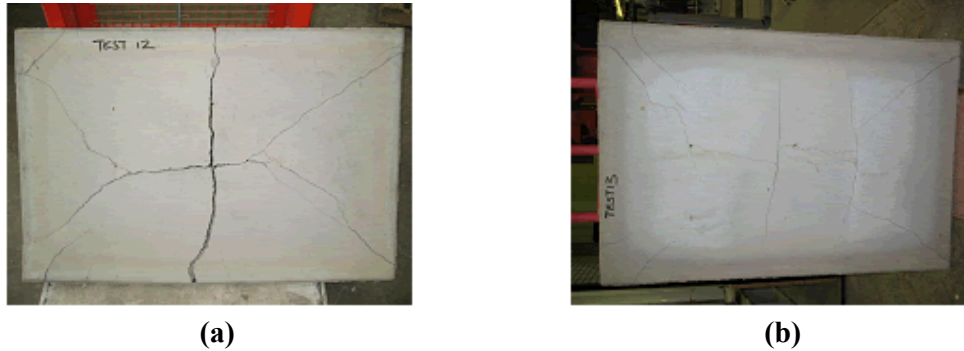


FIGURE 9 : View of bottom of slab; (a) Test 12, (b) Test 13 after testing.

It was apparent that, for the slab reinforced with deformed wire, once the major tension crack had formed across the short span the reinforcement across the crack fractured. Because of the better bond achieved between the concrete and steel in this case, the straining of the reinforcement occurs over a smaller free length and fracture strains happen at quite small crack widths. In Test 12, as the transverse crack developed the reinforcing bars across the tension crack were also exposed to the high temperatures, and would fracture progressively in an “unzipping” effect more rapid than in the ambient-temperature tests [10]. This is not apparent in Test 13, in which the smooth wire has not fractured because it does not develop local strains of the same order because the free lengths of wire across the tension crack can become much higher and the strains do not achieve the fracture levels.

DEFLECTIONS

The mid-span vertical deflections of the slabs tested so far are shown in Fig. 10. Some of these have attained deflections up to $Span/12$. The slabs show similar rates of deflection between 20°C-150°C. The slabs of depth 22mm with reinforcement placed 7.5mm from the bottom surface (Tests 9 and 11) deflections are lower than for the 15mm thick slabs. The rate of deflection for the slab reinforced with smooth wire (Test 13) can be seen to be less than for the equivalent slab using deformed wire (Test 12).

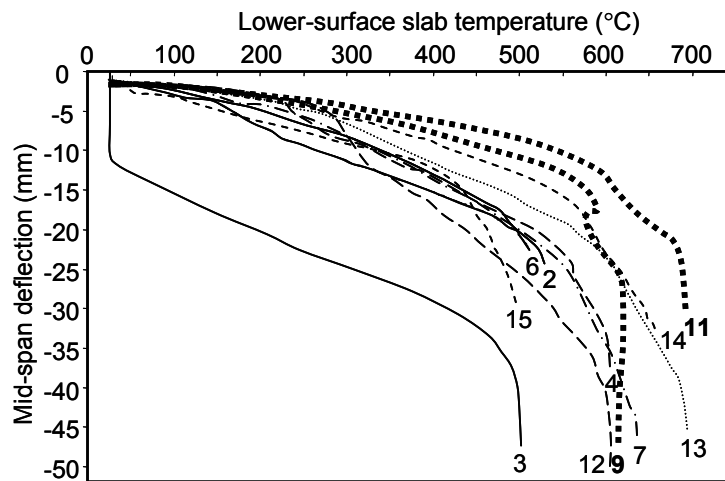


FIGURE 10: Mid-span deflections for the tested slabs (Test numbers indicated).

Some numerical modelling studies have been completed using *Vulcan*, and comparisons are presented in Fig. 11. Mesh studies were undertaken at ambient temperature in order to validate the model. The results show good correlation between test and numerical results. This seems to indicate that, even though the numerical model does not consider the effects of bond strength on reinforcement fracture, it predicts behaviour very similar to that shown in the tests. This work is currently in progress and parametric studies will be carried out.

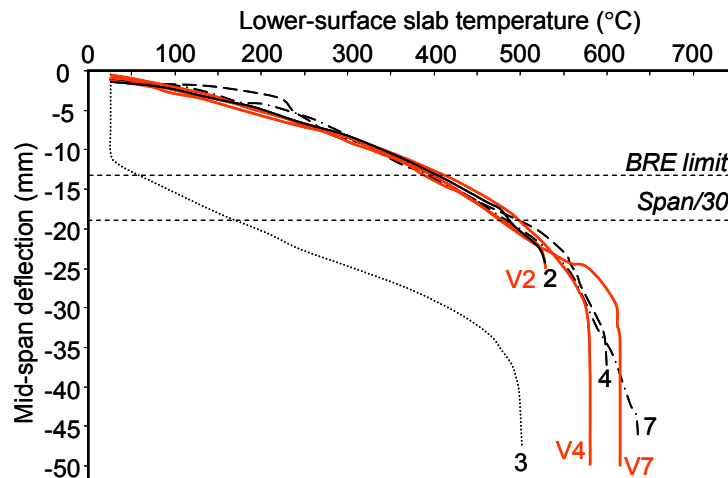


FIGURE 11 : Comparison of experimental results with numerical model *Vulcan*

The maximum displacements calculated using the BRE simple design method give results somewhat below the standard testing deflection limit of *Span/30*. At either of these deflection limits the slabs are all intact, and both limits are clearly conservative.

COMPARISONS WITH THE SIMPLE DESIGN METHOD

A reduced, high-temperature yield-line load capacity can be calculated using the reduced strengths of the reinforcing steel at elevated temperatures. The experimentally measured steel temperatures were used to assign appropriate strength reduction factors from Eurocode 3 Part 1.2 [14]. Fig. 12 plots the enhanced load ratios carried by the slabs in some of the tests in terms of the reduced yield-line capacity, showing that the slabs carried loads far greater than yield line predictions. At displacements greater than 15mm this capacity was demonstrably enhanced by tensile membrane action.

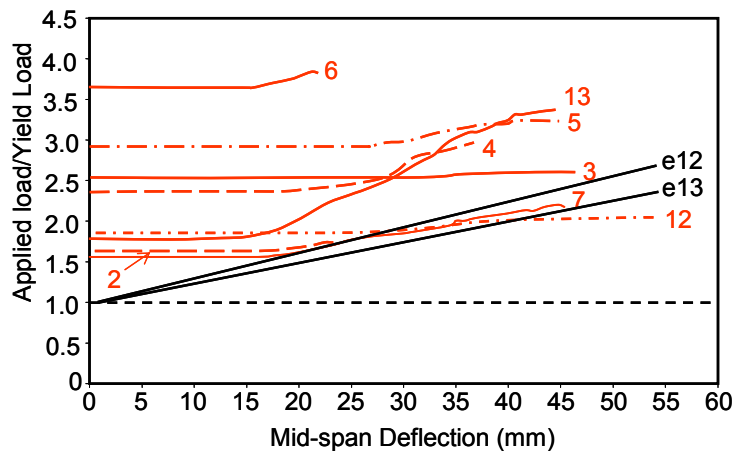


FIGURE 12: Variation of Applied load/Yield load with deflection

In order to compare Tests 12 and 13, the theoretical enhancement factors given by the BRE simple design method are plotted on Fig. 12 as lines e12 and e13 respectively. It can be seen that Test 13, which had smooth reinforcement, actually reached much higher enhancements than predicted by the BRE method. However for Test 12, using deformed reinforcement, the enhancement was close to the prediction within the permitted deflection range, but fell below it for very high deflections. Test 13 reached factors of nearly 3.5 times the yield line load compared to Test 12 which only reached 1.9. Fig. 13 compares the calculated load capacity of the slabs for Tests 12 and 13.

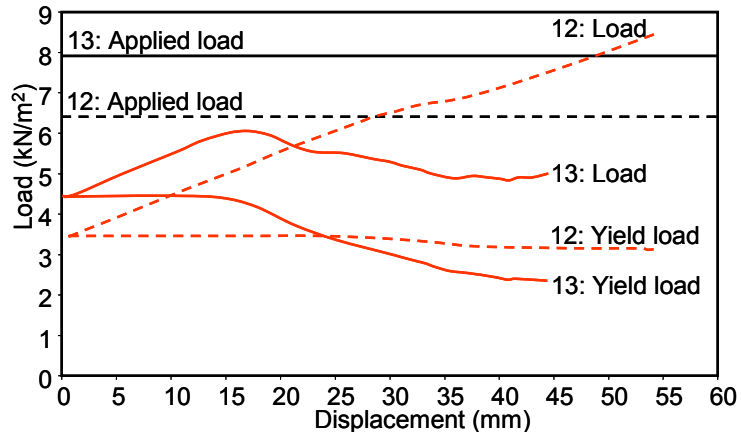


FIGURE 13: Comparison of the load and yield-line capacities for Tests 12 and 13 from the BRE design method with the actual load levels as deflections increase.

Fig. 13 compares the load capacities calculated using the BRE design method, mapping the reinforcement temperatures onto the measured displacements in Tests 12 and 13. These tests differ only in the reinforcement type used. This illustrates again that Test 13, using smooth reinforcement, out-performs the BRE method's predictions throughout the range of deflections used. However, for Test 12 the BRE prediction increases beyond the actual load at about 27mm displacement, indicating that the deformed reinforcement is performing less well.

CONCLUSIONS

The paper presents the results from a number of loaded high-temperature tests conducted on horizontally unrestrained slabs. An electrical heating system and self-supporting frame have been developed to enable the slabs to be heated up to lower-surface temperatures of about 700°C. The slabs have in general performed very well and supported loads well in excess of the predicted yield line loads. Enhancements of up to 3.5 times the yield load have been achieved; this enhanced resistance being attributed to membrane forces which assist in maintaining the structural integrity through diaphragm action. The slabs reinforced with smooth bars performed better than those reinforced with deformed bars.

A major purpose of these tests was to investigate the influence of thermal curvature on the failure mechanisms of rectangular slabs. Observations from the high-temperature tests have shown that the cracking mechanism differs in some respects from that observed at ambient temperature. At ambient temperature four flat facets of the slab rotate about the edge supports and yield line cracks are formed as a low-deflection mechanism which is forced into membrane action at high deflections. At high temperatures the slab initially deflects

into double curvature, generating full-depth cracking across its short span, and may later form a less distinctive yield line mechanism.

The comparisons between the numerical model *Vulcan* and the experiments have shown that *Vulcan* predicts deflections accurately, even though it does not model discrete cracking. Further studies will follow using *Vulcan* to further understand the mechanics involved in the high-temperature slab behaviour.

ACKNOWLEDGMENT

The authors gratefully acknowledge sponsorship of the first author by the Engineering and Physical Sciences Research Council of the United Kingdom, and by Arup Fire Ltd.

REFERENCES

- [1] ‘*The behaviour of multi-storey framed buildings in fire: a European joint research programme*’, British Steel Swinden Technology Centre, 1999.
- [2] BS5950: *Structural use of steelwork in buildings, Part 8 : Code of practice for fire resistance design*, British Standards Institution, London, 1990.
- [3] Park, R. ‘Ultimate strength of rectangular concrete slabs under short-term uniform loading with edges restrained against lateral movement’, *Proc. Institution of Civil Engineers*, 28, (1964) pp125-150.
- [4] Sawczuk, A and Winnicki, L. ‘Plastic behaviour of simply supported reinforced concrete plates at moderately large deflections’, *Int. J. Solids Structures*, 1, (1965) pp97-111.
- [5] Hayes, B., ‘Allowing for membrane action in the plastic analysis of rectangular reinforced concrete slabs’, *Magazine of Concrete Research*, 20 (65), (1968) pp205-212
- [6] Park, R., ‘Tensile membrane behaviour of uniformly loaded rectangular reinforced concrete slabs with full restrained edges’, *Magazine of Concrete Research*, 16 (46), (1964) pp39-44.
- [7] Brotchie, J.F and Holley, M.J., *Membrane action in slabs: Cracking, deflection, and ultimate load of concrete slab systems*. Publications SP-30, American Concrete Institute, Detroit, Paper 30-16, (1971) pp345-377.
- [8] Bailey, C.G., *Design of steel structures with composite slabs at the fire limit state*. BRE Final Report to the Department of the Environment, Transport and Regions, Building Research Establishment, Garston, UK, 2000.
- [9] Bailey, C.G, ‘Efficient arrangement of reinforcement for membrane behaviour of composite floor slabs in fire conditions’. *J. Construct. Steel Research*, 59, (2003) pp931-949

- [10] Foster, S.J., Bailey, C.G., Burgess, I.W. and Plank, R.J., ‘ *Experimental behaviour of concrete floor slabs at large displacements*’, Research Report DCSE/03/F/2, University of Sheffield (2003), (accepted for publication: *Engineering Structures*).
- [11] Huang, Z, Burgess, I.W. and Plank R.J., ‘Modelling membrane action of concrete slabs in composite buildings in fire: Part I: Theoretical development’. *Journal of Structural Engineering*, ASCE, **129** (8), (2003) pp1093-1102.
- [12] Huang, Z, Burgess, I.W. and Plank R.J., ‘Modelling membrane action of concrete slabs in composite buildings in fire: Part II: Validations. *Journal of Structural Engineering*, ASCE, **129** (8), (2003) pp1103-1112.
- [13] Eurocode 4, *Design of composite steel and concrete structures: Part 1.2: Structural rules, Structural fire design, prEN 1994-1-2*. European Committee for Standardisation, 2003.
- [14] Eurocode 3, *Design of steel structures: Part 1.2: General rules, Structural fire design, prEN 1993-1-2*. European Committee for Standardisation, 2003.

APPENDIX

TABLE 1: Data for the high-temperature slab tests.

Test	Size (mm)	Reinf. Area (%)	t (mm)	f_y (N/mm ²)	Bar Type	f_c (N/mm ²)	Dx (mm)	Dy (mm)	Yield Line Capacity W_u (kN/m ²)	Imposed Load Q (kN/m ²)	Load Ratio Q/W_u
2	850x550	0.15	14	260	smooth	37	6.645	7.355	1.91	2.95	1.5
3	850x550	0.15	14	260	smooth	37	6.645	7.355	1.91	4.60	2.4
4	850x550	0.15	15	260	smooth	37	7.145	7.855	2.06	4.66	2.3
5	850x550	0.15	13	245	deformed	40	6.145	6.855	1.58	4.73	3.0
6	850x550	0.05	14	260	smooth	44	6.645	7.355	0.78	2.67	3.4
7	850x550	0.15	17	245	deformed	40	8.145	8.855	2.21	3.30	1.5
8	850x550	0.1	24	260	smooth	39	16.145	16.855	4.6	4.0	0.9
9	850x550	0.1	23	245	deformed	42	16.045	16.755	4.32	6.0	1.4
10	850x550	0.05	24	245	deformed	39	16.145	16.855	2.49	4.7	1.9
11	850x550	0.05	23	260	smooth	39	15.145	15.855	2.48	5.96	2.4
12	850x550	0.25	14.5	245	deformed	38	6.745	7.455	3.65	6.8	1.9
13	850x550	0.25	16	260	smooth	38	8.145	8.855	4.68	6.8	1.5
14	850x550	0.1	14.5	245	deformed	40	6.845	7.555	1.25	2.5	2.0
15	850x550	0.05	13.95	260	smooth	40	6.62	7.33	0.77	1.69	2.2